JOURNAL OF THE AMERICAN COLLEGE OF CARDIOLOGY VOL. 73, NO. 7, 2019

Serial Magnetic Resonance Imaging to Identify Early Stages of Anthracycline-Induced Cardiotoxicity

Carlos Galán-Arriola, DVM,[a,b] Manuel Lobo, MD,[a,c] Jean Paul Vílchez-Tschischke, MD,[a,c] Gonzalo J. López, RT,[a] Antonio de Molina-Iracheta, DVM,[a] Claudia Pérez-Martínez, DVM, PhD,[d] Jaume Agüero, MD, PhD,[a,b,e] Rodrigo Fernández-Jiménez, MD, PhD,[a,b,f] Ana Martín-García, MD, PhD,[b,g] Eduardo Oliver, PhD,[a] Rocío Villena-Gutierrez, MBs,[a] Gonzalo Pizarro, MD, PhD,[a,b,c] Pedro L. Sánchez, MD, PhD,[b,g] Valentin Fuster, MD, PhD,[a,f] Javier Sánchez-González, PhD,[h] Borja Ibanez, MD, PhD[a,b,i]

ABSTRACT

BACKGROUND Anthracycline-induced cardiotoxicity is a major clinical problem, and early cardiotoxicity markers are needed.

OBJECTIVES The purpose of this study was to identify early doxorubicin-induced cardiotoxicity by serial multiparametric cardiac magnetic resonance (CMR) and its pathological correlates in a large animal model.

METHODS Twenty pigs were included. Of these, 5 received 5 biweekly intracoronary doxorubicin doses (0.45 mg/kg/injection) and were followed until sacrifice at 16 weeks. Another 5 pigs received 3 biweekly doxorubicin doses and were followed to 16 weeks. A third group was sacrificed after the third dose. All groups underwent weekly CMR examinations including anatomical and T_2 and T_1 mapping (including extracellular volume [ECV] quantification). A control group was sacrificed after the initial CMR.

RESULTS The earliest doxorubicin-cardiotoxicity CMR parameter was T_2 relaxation-time prolongation at week 6 (2 weeks after the third dose). T_1 mapping, ECV, and left ventricular (LV) motion were unaffected. At this early time point, isolated T_2 prolongation correlated with intracardiomyocyte edema secondary to vacuolization without extracellular space expansion. Subsequent development of T_1 mapping and ECV abnormalities coincided with LV motion defects: LV ejection fraction declined from week 10 (2 weeks after the fifth and final doxorubicin dose). Stopping doxorubicin therapy upon detection of T_2 prolongation halted progression to LV motion deterioration and resolved intracardiomyocyte vacuolization, demonstrating that early T_2 prolongation occurs at a reversible disease stage.

CONCLUSIONS T_2 mapping during treatment identifies intracardiomyocyte edema generation as the earliest marker of anthracycline-induced cardiotoxicity, in the absence of T_1 mapping, ECV, or LV motion defects. The occurrence of these changes at a reversible disease stage shows the clinical potential of this CMR marker for tailored anthracycline therapy. (J Am Coll Cardiol 2019;73:779–91) © 2019 The Authors. Published by Elsevier on behalf of the American College of Cardiology Foundation. This is an open access article under the CC BY-NC-ND license (http://creativecommons.org/licenses/by-nc-nd/4.0/).

Anthracyclines are highly effective and frequently used chemotherapy drugs (1), with the most commonly used being doxorubicin, alone or in combination with other anticancer agents. A prominent undesired effect of anthracycline therapy is cardiotoxicity and subsequent heart failure; depending on the accumulated dose, the incidence of severe anthracycline-induced cardiotoxicity resulting in overt systolic heart failure can be as high as 25% (2). The trade-off between

Listen to this manuscript's audio summary by Editor-in-Chief Dr. Valentin Fuster on JACC.org.

From the [a]Centro Nacional de Investigaciones Cardiovasculares (CNIC), Madrid, Spain; [b]Centro de Investigación Biomédica en Red en Enfermedades Cardiovasculares (CIBERCV), Madrid, Spain; [c]Complejo Hospitalario Ruber Juan Bravo, Madrid, Spain; [d]Facultad de Veterinaria de León, León, Spain; [e]Cardiology Department, Hospital Universitari i Politecnic La Fe, Valencia, Spain; [f]Zena and Michael A. Wiener Cardiovascular Institute, Icahn School of Medicine at Mount Sinai, New York, New York; [g]Cardiology Department, Hospital Universitario de Salamanca-IBSAL, Salamanca, Spain; [h]Philips Healthcare, Madrid, Spain; and the [i]Cardiology Department, IIS-Fundación Jiménez Díaz Hospital, Madrid, Spain. This study was partially supported by grants from the Ministerio de Ciencia, Innovación y Universidades through the Carlos III Institute of Health-Fondo de Investigación Sanitaria (PI16/02110), the European Regional Development Fund (SAF2013-49663-EXP), and the Spanish Society of Cardiology (FEC basic

ISSN 0735-1097 https://doi.org/10.1016/j.jacc.2018.11.046

ABBREVIATIONS AND ACRONYMS

CMR = cardiac magnetic resonance

ECV = extracellular volume

LAD = left anterior descending coronary artery

LV = left ventricular

LVEF = left ventricular ejection fraction

MOLLI = T_1 modified Look-Locker Inversion recovery sequence

cancer and chronic heart failure places an immense personal burden on patients, with physical and psychological consequences.

Anthracyclines bind to topoisomerase 2β in the cardiomyocyte's DNA. Anthracyclines-topoisomerase 2β complexes bind to promoters of mitochondrial antioxidative, biogenesis, and electron transport chain genes leading to a downstream mitochondrial dysfunction. In fact, genetic ablation of topoisomerase 2β in mice ameliorates anthracycline-induced cardiotoxicity (3). In addition, anthracyclines bind to cardiolipin in the inner mitochondrial membrane, contributing to increased reactive oxygen species generation, iron deposition, and defective mitochondrial biogenesis (3,4). Altogether, these phenomena lead to mitochondrial swelling, intracardiomyocyte vacuolization, and ultimately, cell death and replacement of cardiomyocytes by fibrotic tissue (5–7).

SEE PAGE 792

Current algorithms to identify early stages of anthracycline-induced cardiotoxicity are far from optimal. Diagnosis generally occurs once left ventricular (LV) functional deterioration becomes manifest, either as a decline in left ventricular ejection fraction (LVEF) or longitudinal LV strain abnormalities (8,9). By this stage, the damage to the myocardium is often irreversible. The lack of a validated early damage marker limits the development of preventive strategies. Cardiac magnetic resonance (CMR) is the gold standard technique for anatomical and functional evaluation of the heart, and the advent of multiparametric algorithms allows accurate characterization of myocardial tissue. CMR is thus suitable for the detection of myocardial edema (10–12) and diffuse myocardial fibrosis (13–15), which are present at different stages of anthracycline-induced cardiotoxicity (16–21). To date, there has been a lack of comprehensive serial multiparametric CMR tissue studies characterizing the full anthracycline treatment cycle from pre-treatment, through treatment, to overt LV systolic dysfunction and heart failure.

Here, we used a large animal model (pig) of doxorubicin-induced cardiotoxicity to identify the earliest CMR marker of myocardial damage and its pathological correlates. We also studied the reversibility of cardiotoxicity upon detection of the early CMR marker.

METHODS

STUDY DESIGN. The study was approved by the Institutional Animal Research Committee and conducted in accordance with recommendations of the Guide for the Care and Use of Laboratory Animals. The study design is summarized in **Figure 1**. The study population consisted of 20 castrated male large white pigs (25 to 35 kg). Pigs in group 1 received 5 biweekly doxorubicin injections (final injection at week 8) and were followed-up until sacrifice at week 16 by intravenous injection of pentobarbital sodium in overdose. In group 2, pigs underwent 3 biweekly doxorubicin injections (final injection at week 4) and were similarly followed-up until sacrifice at week 16. Group 3 pigs underwent the same doxorubicin protocol as group 2 (3 biweekly injections) but were sacrificed earlier, at week 6 (2 weeks after the final doxorubicin injection). Group 4 was a control group sacrificed after baseline CMR without doxorubicin exposure. In all groups, weekly comprehensive multiparametric CMR examinations were performed until sacrifice. In the treatment weeks, CMR scans were performed immediately before doxorubicin injections.

DOXORUBICIN ADMINISTRATION PROCEDURE. We used a modification of a previously described approach (22,23). Animals were anesthetized and endotracheally intubated. The femoral artery was then accessed by the Seldinger technique, and a 7-F sheath was inserted. Pigs were anticoagulated with 150 IU/kg of intravenous heparin, and a 5-F coronary diagnostic catheter was inserted via a femoral sheath and placed at the origin of the left coronary artery. Under angiography guidance, a 0.014-mm coronary guidewire was positioned distally in the left anterior descending (LAD) coronary artery. The catheter was

science in cardiology grant). This research program is part of an institutional agreement between the CNIC and FIIS-Fundación Jiménez Díaz. This study forms part of a Master Research Agreement between the CNIC and Philips Healthcare, and is part of a bilateral research program between Hospital de Salamanca Cardiology Department and the CNIC. The CNIC is supported by the Ministerio de Ciencia, Innovación y Universidades, and the Pro-CNIC Foundation, and is a Severo Ochoa Center of Excellence (MEIC award SEV-2015-0505). Drs. Galán-Arriola and Villena-Gutierrez are P-FIS fellows (Instituto de Salud Carlos III). Dr. Fernández-Jiménez has received funding through the European Union Horizon 2020 Research and Innovation program under grant MSCA-IF-GF-707642. Dr. Sánchez-González is an employee of Philips Healthcare. All other authors have reported that they have no relationships relevant to the contents of this paper to disclose.

Manuscript received August 13, 2018; revised manuscript received October 14, 2018, accepted November 8, 2018.

FIGURE 1 Study Design

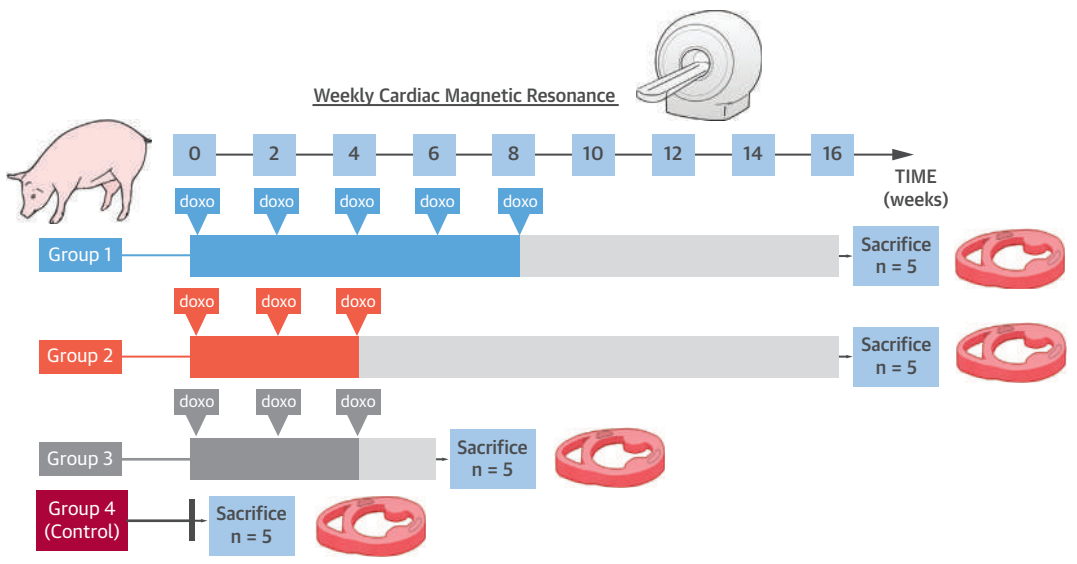

Large white castrated male pigs weighing 25 to 30 kg were used in this study. Animals were divided into 4 experimental groups of 5 animals each. Group 1 animals received 5 biweekly intracoronary (IC) doxorubicin (doxo) doses followed by 8 dose-free weeks, whereas Group 2 pigs received 3 biweekly IC doxo doses followed by 12 dose-free weeks. Group 3 pigs received 3 IC doxo dose followed by 2 dose-free weeks before sacrifice. Group 4 was a control group of untreated animals. Cardiac magnetic resonance scans were performed every week in each group, before doxo infusion. Infused and remote myocardial areas were collected at sacrifice for further analysis.

docked selectively in the LAD, and a 0.45 mg/kg dose of doxorubicin (Farmiblastina, Pfizer, New York, New York) diluted in 30 ml saline was given as a slow bolus injection over 3 min. Electrocardiographic and hemodynamic monitoring was maintained during doxorubicin administration. Once the infusion was completed, coronary angiography was performed to document normal coronary flow, the catheter material was removed, and the animal was allowed to recover.

CMR PROTOCOL. All studies were performed with a Philips 3-T Achieva Tx whole body scanner (Philips Healthcare, Best, the Netherlands) equipped with a 32-element phased-array cardiac coil. The CMR protocol included a standard segmented cine steady-state free-precession sequence to provide high-quality anatomical references, a T_2 gradient-spin-echo mapping sequence, and native and post-contrast T_1 mapping and late gadolinium enhancement (LGE) sequences.

The imaging parameters for the standard segmented cine steady-state free-precession sequence were as follows: field of view (FOV) of 280 × 280 mm, slice thickness 6 mm with no gaps, repetition time (TR) 2.8 ms, echo time (TE) 1.4 ms, flip angle 45°, cardiac phases = 30, voxel size 1.8 × 1.8 mm, and number of excitations = 3. The imaging parameters for the T_2-gradient-spin-echo mapping sequence mapping were FOV 300 × 300 mm with an acquisition voxel size of 1.8 × 2.0 mm^2 and slice thickness 8 mm, and 8 echo times ranging from 6.7 to 53.6 ms. To reduce T_1 effects, a 2-heartbeat interval was used between excitations. The T_1 mapping sequence (Modified Look-Locker Inversion recovery [MOLLI]) was acquired before and 10 min after contrast administration. All MOLLI sequences were based on a 5(3)3 scheme using a single shot steady-state free precession readout sequence (TR/TE/flip angle = 2.1 ms/1.05 ms/35°) with an in-plane acquisition resolution of 1.5 × 1.8 mm^2 and an 8-mm slice thickness. T_2 and T_1 mapping sequences were both triggered at mid-diastole and acquired from a single short-axis midapical slice.

LGE imaging was performed 15 min after intravenous administration of 0.2 mmol/kg gadopentetate dimeglumine contrast agent using an 3-dimensional inversion-recovery spoiled turbo field echo sequence (TR/TE/flip angle = 2.4 ms/1.13 ms/10°) with an isotropic resolution of 1.5 × 1.5 × 1.5 mm^3 on a FOV of 340 × 340 × 320 mm^3 in the FH, LR, and AP directions. Data were acquired in mid-diastole with a 151.2-ms acquisition window. Acquisition was accelerated using a net SENSE factor of 2.25 (1.5 × 1.5 in the

AP and LR directions) with a bandwidth of 853 Hz per pixel. Inversion time was adjusted before acquisition using a look-locker scout sequence with different inversion times to ensure proper nulling of the healthy myocardium signal. For the analysis, 3-dimensional volume was reconstructed in short-axis, 2-chamber, and 4-chamber views with a slice thickness of 6 mm.

CMR analysis. CMR studies were analyzed by 2 experienced and independent observers using dedicated software (MR extended Work Space 2.6, Philips Healthcare; and Qmass MR 7.6, Medis, Leiden, the Netherlands). T_2 maps were automatically generated on the acquisition scanner by fitting the signal intensity of all echo times to a monoexponential decay curve at each pixel with a maximum likelihood expectation maximization algorithm. T_1 maps were generated using a maximum-likelihood expectation-maximization algorithm and fitting the MR signal to a T_1 inversion recovery with 3 independent model parameters. T_2 and T_1 relaxation maps were quantitatively analyzed by placing a wide transmural region of interest at the infused myocardial area (irrigated by the LAD) of the corresponding slice in all studies. Delayed gadolinium-enhanced regions were defined as >50% of maximum myocardial signal intensity (full width at half maximum) and qualitatively analyzed. Extracellular volume (ECV) was estimated with native T_1-MOLLI values and 10-min post-contrast T_1-MOLLI values corrected by hematocrit, as described elsewhere (13).

Ex-vivo analysis. After heart extraction, samples of the doxorubicin-infused region (anteroseptal wall) and the remote area were collected for histology and water content quantification. For histological studies, samples were fixed in 4% formalin and then transferred to 70% ethanol. After paraffin embedding, 4-μm sections were cut and stained with hematoxylin and eosin, Masson trichrome, and Sirius Red. Stained sections were scanned, and 20 × 20 magnification images were taken for collagen quantification using a modified macro (24).

For water content quantification, harvested tissue samples were immediately blotted to remove surface moisture and then introduced into laboratory crystal containers previously weighed on a high-precision scale. The tissue-loaded containers were weighed before and after drying for 48 h at 100°C in a desiccating oven. Tissue water content (% dry weight) was calculated using the following formula: water content = ([wet weight − dry weight]/dry weight) × 100. An empty container was weighed before and after desiccation as an additional calibration control.

STATISTICAL ANALYSIS. Sample size selection. Objective 1 was hypothesis generating, and for this reason, we used an arbitrary same sample size of 5 animals (similar to previous hypothesis-generating pig studies [25]). For objective 2, we based the sample size selection on results (T_2 relaxation times) from objective 1, and on the capacity to detect a meaningful 5-ms difference in T_2 relaxation time between examination time points. Taking into consideration an anticipated SD of 3 ms, and multiple pairwise comparisons between time points, a sample size of 5 individuals/group resulted in a statistical power of 80% to detect differences.

Variables are expressed as mean ± SD or median (interquartile range [Q1, Q3]) as appropriate. Data normality was assessed with the Shapiro-Wilk test.

The Student's *t*-test was used for 2-group comparisons, and the changes of imaging variables across time was assessed using 1-way repeated measures analysis of the variance test. To identify the timepoints showing statistically significant changes compared with the baseline values, pairwise paired Student's *t*-tests were performed taking into account p value adjustment for multiple comparisons (Bonferroni method). Differences were considered statistically significant at $p < 0.05$. All data were analyzed with RStudio (RStudio Team [2015], Integrated Development for RStudio, Inc., Boston, Massachusetts), and graphics were created with ggplot2.

RESULTS

None of the pigs showed adverse events during doxorubicin administration at any time point (i.e., no changes were noted in electrocardiogram or systolic arterial pressure during injections). None of the pigs died during the study.

SERIAL CMR TISSUE CHARACTERIZATION OF DOXORUBICIN-INDUCED CARDIOTOXICITY. A total of 5 pigs received 5 biweekly doxorubicin injections (weeks 0, 2, 4, 6, and 8). Multiparametric CMR was performed weekly until week 16, when animals were sacrificed and hearts were harvested for pathology evaluation.

LV ejection fraction. Weekly CMR examinations revealed no changes in LVEF until week 9 (1 week after the fifth and final doxorubicin injection). From week 9 onwards, LVEF declined progressively, the decline becoming significant at week 12 (55 ± 4% at baseline vs. 33 ± 6% at week 12; $p < 0.01$). The lowest LVEF value was recorded at the 16-week time point (30 ± 8%; $p = 0.01$ vs. baseline). Group and

FIGURE 2 **Animal Model of Anthracycline Cardiotoxicity (Group 1)**

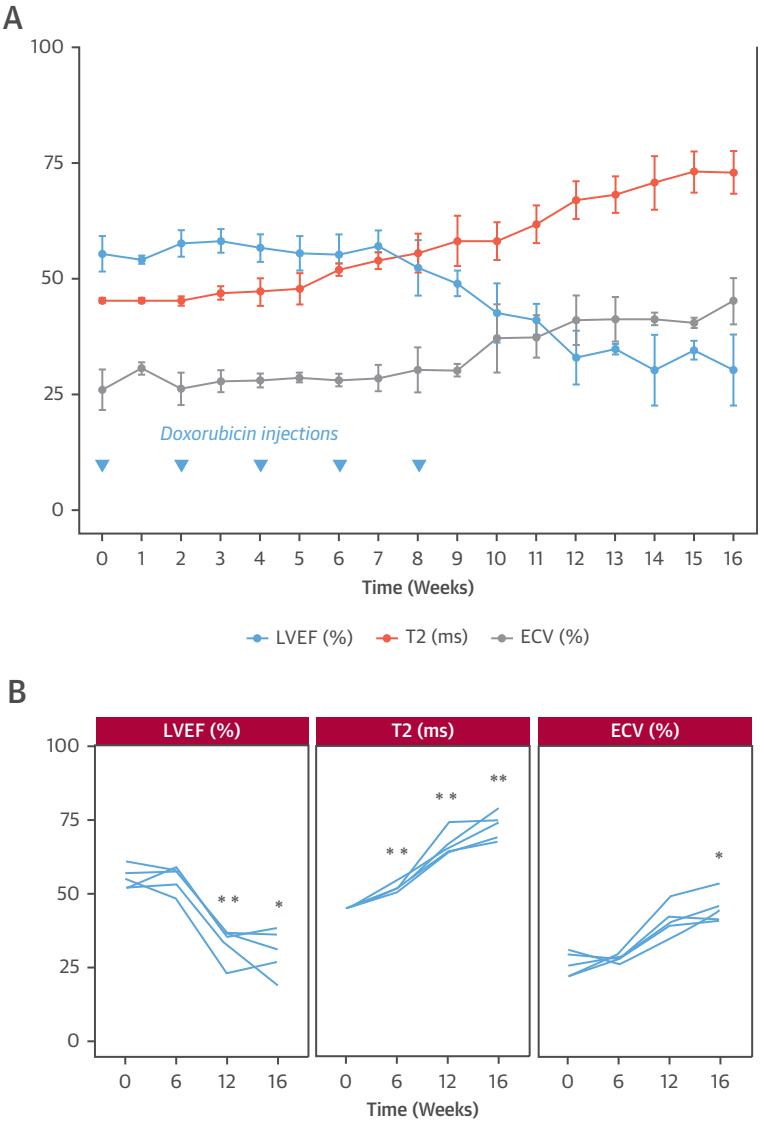

(A) Time course of cardiac magnetic resonance (CMR) imaging studies. Data are represented as mean ± SD **(bars). (B)** Individual animal data at selected time points for left ventricular ejection fraction (LVEF), T_2, and extracellular volume (ECV). **Asterisks** indicate statistically significant differences compared with week 0: *p < 0.05, **p < 0.01.

individual LVEF trajectories are presented in **Figures 2A and 2B**. LVEF data are presented in Online Table 1. In agreement with the LVEF data, no regional contractile abnormalities were documented until week 12, when the doxorubicin-infused myocardium showed regional wall motion defects (data not shown).

T_2 relaxation times. Weekly CMR examinations revealed no changes in T_2 relaxation times on CMR examinations performed at weeks 0 through 5. At week 6, T_2 relaxation times were significantly longer than at baseline (45.2 ± 0.5 ms and 52.0 ± 1.4 ms at baseline and week 6, respectively; p = 0.007). T_2 relaxation times subsequently increased, reaching a maximum at end follow-up (73.0 ± 4.6 ms and 72.8 ± 4.6 ms on weeks 12 and 16; p = 0.003 and p = 0.001 vs. baseline, respectively). Group and individual T_2 trajectories are presented in **Figures 2A and 2B**. T_2 relaxation times at all time points are presented in Online Table 1.

FIGURE 3 Time Course CMR Comparison Between Groups 1 and 2

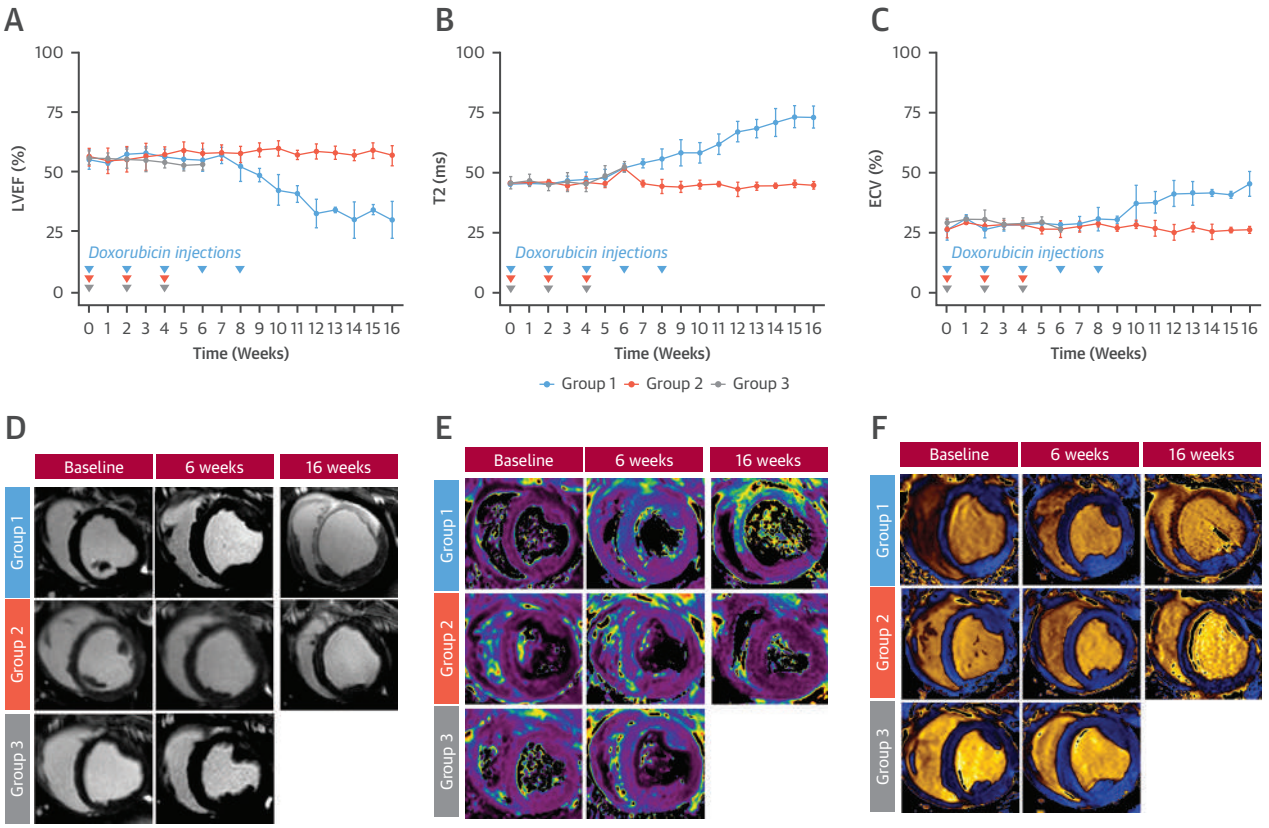

(A) LVEF (%). **(B)** T_2-gradient-spin-echo (T_2-GraSE) mapping sequence in the infused area (in ms). **(C)** ECV in the infused area (%). **(D)** Representative images of late gadolinium enhancement sequences for selected time points and groups. **(E)** Representative images of T_2-GraSE mapping for selected time points and groups, represented with a masked range (20 to 120 ms). **(F)** Representative images of native T_1-MOLLI mapping for selected time points and groups, represented with a masked range (550 to 1,750 ms). Abbreviations as in Figure 2.

T_1 relaxation times. Native T_1 relaxation times showed no change from baseline until week 10 (2 weeks after the fifth and final doxorubicin dose). A nonsignificant increase was noted at week 10, followed by a progressive increase to end follow-up at week 16. Native T_1 values were significantly longer than at baseline only from week 12 onwards (1,087 ± 101 ms and 1,220 ± 59 ms at baseline and week 12 respectively; $p = 0.02$). Group and individual native T_1 trajectories are presented in Online Figures 1A and 1C. Complete T_1 relaxation time data are presented in Online Table 1.

Extracellular volume. ECV expansion was tracked using a validated formula that includes pre- and post-contrast T_1 values and hematocrit (13). In parallel with the native T_1 trajectory, ECV did not differ from baseline until week 10 (2 weeks after the fifth and final doxorubicin dose). ECV subsequently expanded progressively, but with no statistically significant difference from baseline until week 14 (26.03 ± 5.81% and 41 ± 1.34% at baseline and week 14, respectively; $p = 0.006$). Group and individual ECV trajectories are presented in Figures 2A and 2C. Complete ECV data are presented in Online Table 1. Post-contrast T_1 relaxation times are presented in Online Figures 1B and 1C.

Late gadolinium enhancement. Positive LGE areas first appeared in the doxorubicin-infused area from week 10 onwards. The enhanced areas formed a patchy pattern at week 12, becoming more evident at 16 weeks follow-up (Figure 3D).

T_2-DRIVEN STRATEGY FOR THE PREVENTION OF ANTHRACYCLINE-INDUCED CARDIOTOXICITY. Having documented T_2 mapping abnormalities preceding systolic function deterioration, we next explored whether T_2 relaxation time prolongation occurred at a

reversible stage of anthracycline-induced cardiotoxicity. To address this question, we studied a group of 5 pigs (group 2) in which doxorubicin treatment was stopped upon detection of T_2 prolongation. As in group 1, T_2 relaxation times in group 2 pigs were nonsignificantly prolonged at week 5 and this prolongation became significant at week 6 (i.e., immediately before the scheduled fourth doxorubicin dose). Group 2 pigs therefore received only 3 doxorubicin doses (weeks 0, 2, and 4) and were followed-up until week 16. T_2 relaxation times in group 2 pigs were significantly prolonged at week 6 (45.6 ± 0.6 ms and 51.6 ± 0.8 ms at baseline and week 6, respectively; $p = 0.004$) but returned to baseline levels at week 8 (45.5 ± 1.3 ms; $p = 1.00$ vs. baseline), and these levels were maintained until the end of follow-up (44.8 ± 1.4 ms at week 16; $p = 1.00$ vs. baseline) (**Figure 3B and 3E**, red lines). LVEF in group 2 showed no deterioration during follow-up (**Figure 3A**), and regional LV wall motion was similarly unaffected. All other evaluated parameters in group 2 remained within normal ranges throughout follow-up (**Figure 3**, red lines, and Online Table 1).

PATHOLOGICAL CORRELATES OF EARLY T_2 MAPPING CHANGES. The underlying tissue composition changes leading to early T_2 relaxation-time prolongation in the presence of normal T_1 and ECV readings was investigated in another group of 5 pigs (Group 3). Group 3 animals received 3 doxorubicin doses at weeks 0, 2, and 4, and were sacrificed immediately after detection of T_2 prolongation (at week 6). Like the other groups, these animals underwent a weekly CMR examination. Tissue samples from group 3 animals were compared with samples from groups 1 and 2 animals, which were sacrificed at the end of the 16-week protocol.

Myocardial water content. As expected, T_2 relaxation-time prolongation was associated with an increase in myocardial water content (10). At week 6, after 3 doxorubicin doses, T_2 relaxation times were significantly prolonged in group 3 animals (45.8 ± 2.52 ms and 52.6 ± 2.2 ms at baseline and week 6, respectively; $p = 0.01$) (**Figures 3B and 3E**, gray lines). Myocardial water content was significantly elevated in samples harvested at this time point (396 ± 12% of dry weight and 375 ± 0.7% in group 3 and control, respectively; $p = 0.014$) (**Figure 4C**). ECV CMR data for group 3 revealed no expansion of the extracellular space at week 6 (**Figures 3C and 3F**, gray line), indicating that the increased myocardial water content and T_2 prolongation likely corresponds to intracellular edema.

At the end of follow-up in group 1 (5 biweekly doxorubicin doses followed by sacrifice at week 16), myocardial water content was also significantly increased (500 ± 39% of dry weight; $p < 0.001$ vs. control). At this time point, ECV CMR data revealed an overt increase in extracellular space (**Figures 3C and 3F**, blue line), a finding compatible with extracellular edema formation. This is consistent with the positive LGE at this disease stage (**Figure 3D**). Interestingly, myocardial end follow-up water content in group 2 (3 biweekly doxorubicin doses and follow-up to week 16) did not differ from control subjects (365 ± 0.5%; $p = 0.13$ vs. control). Myocardial water content in all groups is shown in **Figure 4C**.

Structural myocardial changes. Hematoxylin and eosin staining of group 3 samples (harvested at week 6, after 3 doxorubicin doses) revealed cardiomyocyte vacuolization (**Figure 4E**, left panel) with no other overt alteration to myocardial tissue structure; cardiomyocytes maintained their shape, and there was no increase in extracellular space. Interestingly, at 16-week follow-up of animals receiving 3 doxorubicin doses (group 2), samples showed no intracardiomyocyte vacuolization (**Figure 4E**, right panel). Conversely, myocardial samples from group-1 pigs (5 doxorubicin doses and 16-week follow-up) showed even larger intracardiomyocyte vacuolae and a disarrayed myocardial structure, with increased extracellular space and replacement fibrosis, suggestive of end-stage disease (**Figures 4A and 4E**, middle panel).

Complete histopathology data (fibrosis, myocardial water content, and vacuolae presence) and CMR data (ECV and T_2 relaxation times) are shown for all groups and sacrifice time points in **Figure 4**.

DISCUSSION

In a pig model of anthracycline-induced cardiotoxicity with serial multiparametric CMR evaluations, we demonstrate that T_2 mapping abnormalities provide the earliest marker of subtle myocardial damage, with T_2 relaxation times prolonged long before LV motion abnormalities were detected (**Central Illustration**). At this early stage of cardiotoxicity, T_1 relaxation times and ECV quantification were unaltered. Pathology evaluation upon T_2 prolongation demonstrated an absolute increase in myocardial water content, correlating with vacuolae formation in preserved cardiomyocytes but with no concomitant fibrosis or increased extracellular space. These findings demonstrate that T_2 relaxation-time prolongation in the presence of normal T_1 mapping and ECV identifies intracardiomyocyte edema as the

FIGURE 4 End Follow-Up Ex Vivo and Imaging Studies of the Infused Area in Each Group

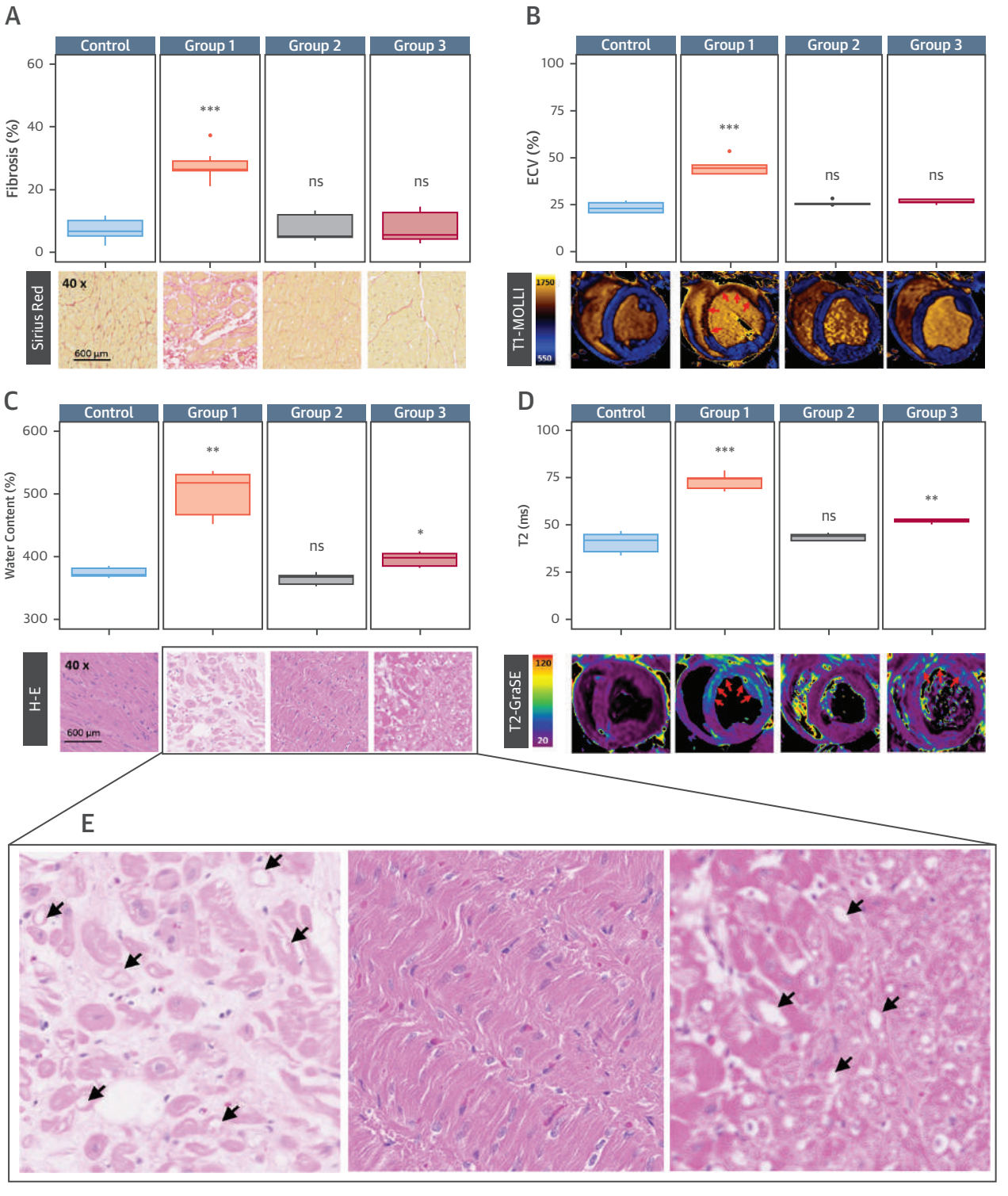

Continued on the next page

earliest anthracycline-induced cardiotoxic event. Our results further demonstrate that stopping doxorubicin administration upon detection of T_2 relaxation-time prolongation prevents progression to myocardial dysfunction, with subsequent T_2 normalization as a surrogate of cardiomyocyte vacuolae resolution. These findings indicate that this marker of intracardiomyocyte edema appears at a reversible disease stage and, thus, has important clinical implications.

Previous CMR evaluations of anthracycline-induced cardiotoxicity have been performed in mice (26), rats (27,28), and rabbits (29,30); however, ours is the first study to use the pig model with serial CMR evaluations. We chose the pig because of its anatomical and physiological similarity to humans (including heart rate and metabolism) and because the CMR protocols are the same as those used clinically. Our study is the most comprehensive to date, because it includes weekly multiparametric CMR evaluations over 4 months to cover all cardiotoxicity stages, from baseline to end-stage disease with overt LVEF deterioration. Following a modification of a published protocol in pigs (22,23), doxorubicin was injected directly into the coronary arteries rather than intravenously. This approach achieves high local doxorubicin concentrations in the heart without exposing animals to undesired systemic adverse effects like myelosuppression, which would render the animals vulnerable to infection and thus potentially affect survival and even cardiac readouts. This approach is validated by the absence of casualties in our study.

Current clinical approaches for the early detection of cardiotoxicity are based on deterioration of LV motion, detected as LVEF or global longitudinal strain (8,9); however, these changes reflect profound damage to myocardial function and thus only become manifest at an advanced stage of the disease. Almost 90% of patients developing anthracycline-mediated LVEF deterioration never fully recover pre-treatment LVEF even with heart failure therapies (31). The identification of T_2 relaxation-time prolongation as a very early marker of reversible intracardiomyocyte vacuolization thus has important clinical implications. Serial T_2 mapping might allow tailored anthracycline dose management, with patients showing no T_2 mapping abnormalities perhaps able to receive further doses, even beyond currently accepted high cardiotoxicity limits, without increasing the risk of future LV dysfunction. This could be especially helpful for patients requiring high anthracycline doses to halt cancer progression. There is also the potential to monitor and possibly modify anthracycline therapy in vulnerable populations, such as patients with pre-existing myocardial disease; pediatric or geriatric patients; smokers; obese or sedentary patients; patients consuming alcohol; or patients with hypertension, diabetes, or hypercholesterolemia (8). The chemotherapy dose-management potential of serial T_2 mapping is supported by the finding that cessation of doxorubicin therapy upon detection of T_2 mapping abnormalities prevented progression to LV motion deterioration or fibrosis development and led to regression of cardiomyocyte vacuolae formation.

Another potential application of serial T_2 mapping is decision making about heart failure therapy initiation (e.g., with beta-blockers and/or ACE inhibitors). This is highly significant, because a major predictor of therapeutic myocardial recovery is the time elapsed between anthracycline therapy and cardiotoxicity diagnosis (32). Cardinale et al. (32) found that only 42% of patients with anthracycline-induced cardiotoxicity fully recovered LV function in response to heart failure therapy; in that study, the percentage of responders decreased progressively as the time from the end of anthracycline therapy to the start of heart failure treatment increased. Therefore, early detection and prompt treatment of cardiotoxicity is crucial to ensuring substantial recovery of cardiac function. With current approaches (based on LVEF and global longitudinal strain), the mean interval from the end of anthracycline therapy to the detection of cardiotoxicity is 3.5 months (31). The ability to identify patients at a much earlier stage would allow earlier initiation of heart failure therapy and would thus prevent many cases of overt LV dysfunction.

FIGURE 4 Continued

Asterisks indicate statistically significant statistical differences compared with week 0 for each time point: *$p < 0.05$, **$p < 0.01$, ***$p < 0.001$, or nonsignificant (NS). **(A)** Fibrosis (%) in the infused area for each group at sacrifice. Representative images show Sirius Red staining. **(B)** ECV (%) in the infused area for each group at sacrifice. Representative images show CMR native T_1-MOLLI with a 550 to 1,750 ms masked range. **Red arrows** mark areas with significantly increased signal. **(C)** Water content (normalized to dry weight) in the infused area for each group at sacrifice. Representative hematoxylin and eosin images are shown. **Black arrows** mark intracardiomyocyte vacuolization. **(D)** T_2-GraSE mapping (ms) in the infused area for each group at sacrifice. Representative images show CMR T_2-GraSE mapping with a 20 to 120 ms mask range. **Red arrows** mark areas with significantly increased signal. Abbreviations as in Figures 2 and 3.

CENTRAL ILLUSTRATION **Serial CMR Evaluations During On-(Anthracycline) Treatment Allows Very Early Detection of Subtle Myocardial Damage**

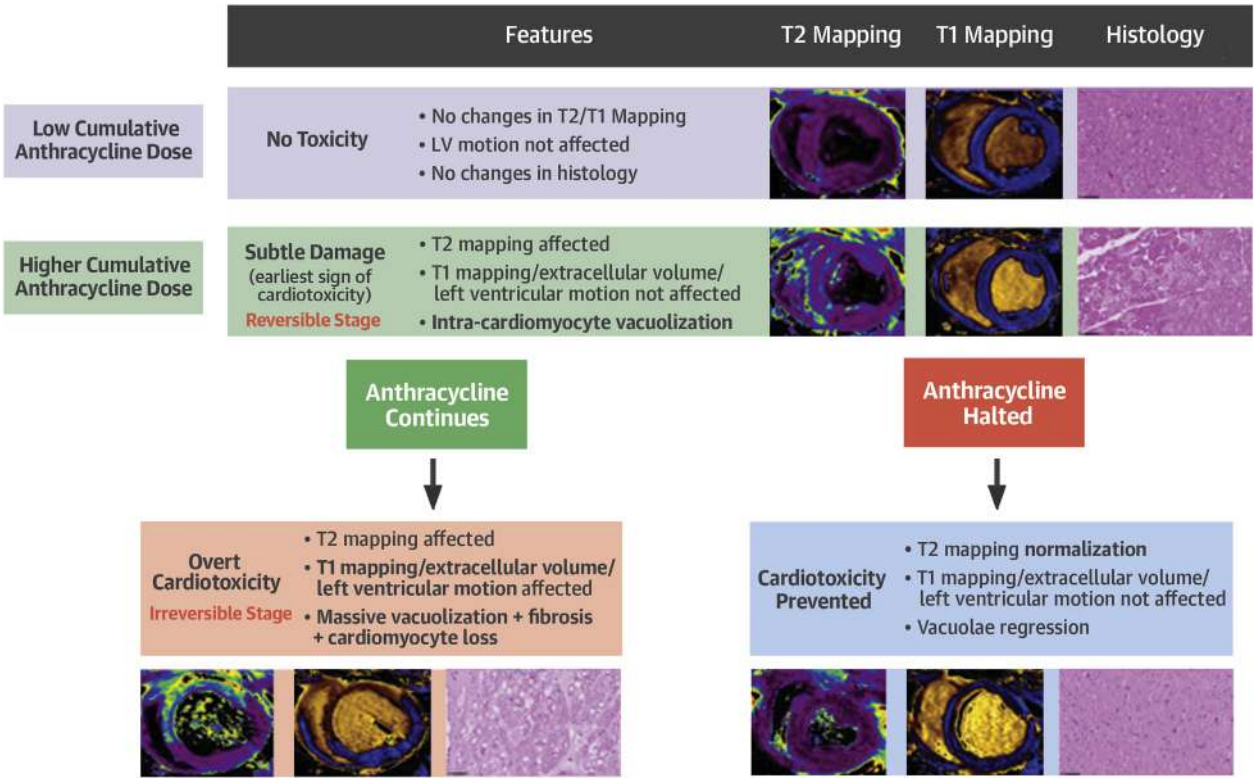

Galán-Arriola, C. et al. J Am Coll Cardiol. 2019;73(7):779–91.

Isolated T_2 relaxation times prolongation (with normal T_1, extracellular volume [ECV], and left ventricular [LV] motion) is able to identify intracardiomyocyte vacuolization, the earliest cardiotoxic event. Stopping anthracycline therapy at this early time point results in no progression to LV motion abnormalities and normalization of T_2 values (corresponding to vacuolae regression). These phenomena support that T_2 mapping identifies anthracycline-induced cardiotoxicity at a reversible stage of the disease. If anthracycline therapy is not halted, T_1 mapping and ECV become pathological at a stage where LV motion is already deteriorated. Serial multiparametric cardiac magnetic resonance (CMR) might serve to implement a personalized treatment approach for patients undergoing anthracycline therapy to prevent cardiotoxicity.

T_2 mapping is an accurate technique for the detection and quantification of myocardial edema (10). We have previously used T_2 mapping to characterize the edematous reaction of porcine (11,25,33) and human (12) myocardium to ischemia/reperfusion. T_2 relaxation time prolongation correlates with increased myocardial water content (10), but by itself does not differentiate between intracellular and extracellular edema. Our multiparametric approach, combining T_2 mapping with T_1 mapping and ECV fraction quantification, here allowed us to define the spatial location of increased myocardial water. T_2 mapping prolongation in the absence of T_1 mapping or T_1-based ECV changes is highly suggestive of intracellular edema formation. Intracellular vacuolization is an early change in the anthracycline-injured myocardium, identified as a pre-apoptotic phenomena in animal models and human biopsies (5-7,34). Our analysis records not only in vivo changes in T_2 mapping, but also the very early presence of intracardiomyocyte vacuolization, before the appearance of LV functional abnormalities. At the end of follow-up in animals undergoing the full doxorubicin protocol (5 biweekly injections and follow-up to 16 weeks), T_2 relaxation times were even longer than at early stages and were accompanied by

significant T_1 relaxation-time prolongation, a significantly elevated T_1-based ECV fraction, and patchy LGE. The pathological correlate at this end-stage of the disease was the presence of larger and more numerous intracardiomyocyte vacuoles accompanied by intense extracellular matrix remodeling and diffuse fibrosis.

Our results are in line with those reported by Farhad et al. (26). Using a mouse model of anthracycline-induced cardiotoxicity, these authors found that 5 weekly doxorubicin injections induced early prolongation of T_2 relaxation times accompanied by intracellular vacuolization (26). This study and ours confirm the feasibility of in vivo noninvasive identification of vacuolae formation inside cardiomyocytes as a direct toxic effect of anthracyclines in 2 different species. However, Farhad et al. (26) found that T_2 mapping abnormalities were associated with concurrent T_1 relaxation-time prolongation and expanded extracellular space on electron microscopy images, a finding not observed in our analysis until later disease stages. This indicates that we identified doxorubicin cardiotoxic effects at an earlier disease stage, when only intracardiomyocyte changes were present, with preservation of the extracellular space. Our weekly protocol was able to identify the onset of cardiac damage, whereas Farhad et al. (26) performed the first scan at the end of the doxorubicin protocol, thus missing the earliest on-treatment tissue composition changes. In another study, Hong et al. (30) used a rabbit model of doxorubicin-induced cardiotoxicity to study the evolution of changes in T_1 mapping and T_1-based ECV, but did not include T_2 mapping. These authors found that T_1 relaxation-time prolongation occurred concurrently with ECV expansion at a time when LVEF had already deteriorated (albeit not significantly vs. baseline). Histological evaluation revealed intracardiomyocyte vacuolization and interstitial fibrosis, indicating that this time point corresponds to more advanced disease stage than that identified by us.

To date, very few studies have used a serial multiparametric CMR strategy including T_2 mapping in patients undergoing anthracycline therapy. Several authors have reported CMR findings in patients treated with anticancer therapies (16–19,35,36). In some of these studies, increased ECV coincided with cardiac function deterioration. Few studies have reported serial CMR examinations before and after anthracycline exposure, and in most of them, CMR was performed only after completion of anthracycline administration, thus missing early changes occurring during treatment (37–40). More recently, Schulz-Menger's group (41) reported the findings of serial multiparametric CMR examinations in a cohort of 30 sarcoma patients on high anthracycline regimes. Patients underwent comprehensive T_2/T_1 mapping and ECV assessment before treatment, 48 h after the first dose, and after finishing the anticancer therapy; 30% of patients developed cardiotoxicity. In contrast with our results, T_2 mapping showed no differences between patients developing cardiotoxicity and those who did not, although both groups showed a nonsignificant trend toward increased T_2 relaxation times over time. ECV did not change over time. Interestingly, patients who subsequently developed cardiotoxicity had significantly shortened T_1 relaxation times 48 h after the first dose. In our study, we observed no drop in T_1 relaxation time after doxorubicin dosing; however, this might reflect the performance of CMR examinations 1 week after dosing in our protocol and not after 48 h as in the study by Muehlberg et al. (41).

Currently, the performance of frequent surveillance, comprehensive, multiparametric, contrast-enhanced CMRs as part of routine care is likely not feasible given the high volume of patients receiving anthracycline-based chemotherapy, high cost, and lack of access to CMR capabilities. We speculate that the development of ultra-fast CMR protocols able to gather the minimum info required for this screening might help alleviate these limitations. In the meantime, this CMR strategy might be offered for those patients at high risk for developing anthracycline-induced cardiotoxicity (8).

STUDY LIMITATIONS. One potential limitation of the present study is the intracoronary doxorubicin administration route, contrasting the intravenous route used in cancer patients. In the pig, the intravenous route requires very high doxorubicin doses that result in significant myelosuppression and compromise the experimental setting (42). The intracoronary approach in the pig model was described by Christiansen et al. (23) and has been validated by several imaging approaches as a valid alternative. In this study, all animals showed a very similar behavior in terms of time to intracardiomyocyte edema and time to LVEF fall. In the clinical setting, this is expected to be more variable. In addition, the time window between T_2 relaxation time prolongation and LVEF fall (3 weeks) appears narrow to be picked-up in the clinical setting. We speculate that this time window might be significantly wider in patients due to the more concealed evolution of the disease but this is to be demonstrated in the clinics.

CONCLUSIONS

In a large animal model of anthracycline-induced cardiotoxicity, we show that the earliest CMR on-treatment event is a prolongation of T_2 relaxation time. T_1 mapping and T_1-based ECV are normal at this early time point and do not change until later in the cardiotoxic process. At this early stage, T_2 mapping abnormalities correspond to intracardiomyocyte edema secondary to doxorubicin-induced vacuolization, unaccompanied by any extracellular alteration. Early identification of intracardiomyocyte edema from T_2 mapping abnormalities has prognostic implications, because stopping doxorubicin treatment upon detection of this early CMR marker stops the progression of LV dysfunction and triggers regression of intracardiomyocyte vacuolization. Serial multiparametric T_2 mapping during treatment has the potential to support personalized anthracycline regimes.

ACKNOWLEDGMENTS The authors thank Eugenio Fernández, Santiago Rodriguez-Colilla, Tamara Córdoba, Óscar Sanz, Nuria Valladares, Inés Sanz, and Rubén Mota for technical and veterinary support at the CNIC animal facility and the farm. They also thank Marta Gavilán, Ángel Macías, and Braulio Pérez for technical support in CMR studies. Simon Bartlett (CNIC) provided English editing.

ADDRESS FOR CORRESPONDENCE: Dr. Borja Ibanez, Translational Laboratory for Cardiovascular Imaging and Therapy, Centro Nacional de Investigaciones Cardiovasculares Carlos III (CNIC), and IIS-Fundación Jiménez Díaz University Hospital, c/ Melchor Fernandez Almagro, 3, 28029 Madrid, Spain. E-mail: bibanez@cnic.es. OR Dr. Javier Sánchez-González, MR Clinical Scientist Philips Healthcare Iberia, c\ María de Portugal, 1, 28050 Madrid, Spain. E-mail: Javier.Sanchez.Gonzalez@philips.com.

PERSPECTIVES

COMPETENCY IN PATIENT CARE AND PROCEDURAL SKILLS: T_2 mapping abnormalities identified by CMR imaging in the presence of normal T_1, ECV, and LV wall motion correlate with cardiomyocyte vacuolization at an early and reversible stage of anthracycline-induced cardiotoxicity.

TRANSLATIONAL OUTLOOK: Prospective trials of chemotherapeutic strategies guided by serial T_2 mapping could incorporate earlier cardiac intervention to preserve ventricular function in those with early cardiotoxicity and higher cumulative anthracycline therapy for those without evidence of toxicity.

REFERENCES

1. Minotti G, Menna P, Salvatorelli E, Cairo G, Gianni L. Anthracyclines: molecular advances and pharmacologic developments in antitumor activity and cardiotoxicity. Pharmacol Rev 2004;56:185–229.

2. Chang HM, Moudgil R, Scarabelli T, Okwuosa TM, Yeh ETH. Cardiovascular complications of cancer therapy: best practices in diagnosis, prevention, and management: part 1. J Am Coll Cardiol 2017;70:2536–51.

3. Zhang S, Liu X, Bawa-Khalfe T, et al. Identification of the molecular basis of doxorubicin-induced cardiotoxicity. Nat Med 2012;18:1639–42.

4. Hahn VS, Lenihan DJ, Ky B. Cancer therapy-induced cardiotoxicity: basic mechanisms and potential cardioprotective therapies. J Am Heart Assoc 2014;3:e000665.

5. Buja LM, Ferrans VJ, Mayer RJ, Roberts WC, Henderson ES. Cardiac ultrastructural changes induced by daunorubicin therapy. Cancer 1973;32:771–88.

6. Friedman MA, Bozdech MJ, Billingham ME, Rider AK. Doxorubicin cardiotoxicity. Serial endomyocardial biopsies and systolic time intervals. JAMA 1978;240:1603–6.

7. Takemura G, Fujiwara H. Doxorubicin-induced cardiomyopathy from the cardiotoxic mechanisms to management. Prog Cardiovasc Dis 2007;49:330–52.

8. Zamorano JL, Lancellotti P, Rodriguez Munoz D, et al. 2016 ESC position paper on cancer treatments and cardiovascular toxicity developed under the auspices of the ESC Committee for Practice Guidelines: The Task Force for Cancer Treatments and Cardiovascular Toxicity of the European Society of Cardiology (ESC). Eur Heart J 2016;37:2768–801.

9. Lopez-Fernandez T, Martin Garcia A, Santaballa Beltran A, et al. Cardio-onco-hematology in clinical practice. Position paper and recommendations. Rev Esp Cardiol (Engl Ed) 2017;70:474–86.

10. Fernandez-Jimenez R, Sanchez-Gonzalez J, Aguero J, et al. Fast T2 gradient-spin-echo (T2-GraSE) mapping for myocardial edema quantification: first in vivo validation in a porcine model of ischemia/reperfusion. J Cardiovasc Magn Reson 2015;17:92.

11. Fernandez-Jimenez R, Garcia-Prieto J, Sanchez-Gonzalez J, et al. Pathophysiology underlying the bimodal edema phenomenon after myocardial ischemia/reperfusion. J Am Coll Cardiol 2015;66:816–28.

12. Fernandez-Jimenez R, Barreiro-Perez M, Martin-Garcia A, et al. Dynamic edematous response of the human heart to myocardial infarction: implications for assessing myocardial area at risk and salvage. Circulation 2017;136:1288–300.

13. Flett AS, Hayward MP, Ashworth MT, et al. Equilibrium contrast cardiovascular magnetic resonance for the measurement of diffuse myocardial fibrosis: preliminary validation in humans. Circulation 2010;122:138–44.

14. Nakamori S, Dohi K, Ishida M, et al. Native T1 mapping and extracellular volume mapping for the assessment of diffuse myocardial fibrosis in dilated cardiomyopathy. J Am Coll Cardiol Intv 2018;11:48–59.

15. Ambale-Venkatesh B, Lima JA. Cardiac MRI: a central prognostic tool in myocardial fibrosis. Nat Rev 2015;12:18–29.

16. Neilan TG, Coelho-Filho OR, Shah RV, et al. Myocardial extracellular volume by cardiac magnetic resonance imaging in patients treated with anthracycline-based chemotherapy. Am J Cardiol 2013;111:717–22.

17. Toro-Salazar OH, Gillan E, O'Loughlin MT, et al. Occult cardiotoxicity in childhood cancer survivors exposed to anthracycline therapy. Circ Cardiovasc Imaging 2013;6:873–80.

18. Ylanen K, Poutanen T, Savikurki-Heikkila P, Rinta-Kiikka I, Eerola A, Vettenranta K. Cardiac

magnetic resonance imaging in the evaluation of the late effects of anthracyclines among long-term survivors of childhood cancer. J Am Coll Cardiol 2013;61:1539–47.

19. Tham EB, Haykowsky MJ, Chow K, et al. Diffuse myocardial fibrosis by T1-mapping in children with subclinical anthracycline cardiotoxicity: relationship to exercise capacity, cumulative dose and remodeling. J Cardiovasc Magn Reson 2013;15:48.

20. Jordan JH, D'Agostino RB Jr., Hamilton CA, et al. Longitudinal assessment of concurrent changes in left ventricular ejection fraction and left ventricular myocardial tissue characteristics after administration of cardiotoxic chemotherapies using T1-weighted and T2-weighted cardiovascular magnetic resonance. Circ Cardiovasc Imaging 2014;7:872–9.

21. Toro-Salazar OH, Lee JH, Zellars KN, et al. Use of integrated imaging and serum biomarker profiles to identify subclinical dysfunction in pediatric cancer patients treated with anthracyclines. Cardiooncology 2018;4:4.

22. Goetzenich A, Hatam N, Zernecke A, et al. Alteration of matrix metalloproteinases in selective left ventricular adriamycin-induced cardiomyopathy in the pig. J Heart Lung Transplant 2009;28:1087–93.

23. Christiansen S, Perez-Bouza A, Schalte G, Hilgers RD, Autschbach R. Selective left ventricular adriamycin-induced cardiomyopathy in the pig. J Heart Lung Transplant 2008;27:86–92.

24. Hadi AM, Mouchaers KT, Schalij I, et al. Rapid quantification of myocardial fibrosis: a new macro-based automated analysis. Cell Oncol (Dordr) 2011;34:343–54.

25. Fernandez-Jimenez R, Galan-Arriola C, Sanchez-Gonzalez J, et al. Effect of ischemia duration and protective interventions on the temporal dynamics of tissue composition after myocardial infarction. Circ Res 2017;121:439–50.

26. Farhad H, Staziaki PV, Addison D, et al. Characterization of the changes in cardiac structure and function in mice treated with anthracyclines using serial cardiac magnetic resonance imaging. Circ Cardiovasc Imaging 2016;9.

27. Cottin Y, Ribuot C, Maupoil V, et al. Early incidence of adriamycin treatment on cardiac parameters in the rat. Can J Physiol Pharmacol 1994;72:140–5.

28. Lightfoot JC, D'Agostino RB Jr., Hamilton CA, et al. Novel approach to early detection of doxorubicin cardiotoxicity by gadolinium-enhanced cardiovascular magnetic resonance imaging in an experimental model. Circ Cardiovasc Imaging 2010;3:550–8.

29. Hong YJ, Kim TK, Hong D, et al. Myocardial characterization using dual-energy CT in doxorubicin-induced DCM: comparison with CMR T1-mapping and histology in a rabbit model. J Am Coll Cardiol Img 2016;9:836–45.

30. Hong YJ, Park HS, Park JK, et al. Early detection and serial monitoring of anthracycline-induced cardiotoxicity using T1-mapping cardiac magnetic resonance imaging: an animal study. Sci Rep 2017;7:2663.

31. Cardinale D, Colombo A, Bacchiani G, et al. Early detection of anthracycline cardiotoxicity and improvement with heart failure therapy. Circulation 2015;131:1981–8.

32. Cardinale D, Colombo A, Lamantia G, et al. Anthracycline-induced cardiomyopathy: clinical relevance and response to pharmacologic therapy. J Am Coll Cardiol 2010;55:213–20.

33. Fernandez-Jimenez R, Sanchez-Gonzalez J, Aguero J, et al. Myocardial edema after ischemia/reperfusion is not stable and follows a bimodal pattern: imaging and histological tissue characterization. J Am Coll Cardiol 2015;65:315–23.

34. Mitry MA, Edwards JG. Doxorubicin induced heart failure: phenotype and molecular mechanisms. Int J Cardiol Heart Vasc 2016;10:17–24.

35. Neilan TG, Coelho-Filho OR, Pena-Herrera D, et al. Left ventricular mass in patients with a cardiomyopathy after treatment with anthracyclines. Am J Cardiol 2012;110:1679–86.

36. Cheung YF, Lam WW, Ip JJ, et al. Myocardial iron load and fibrosis in long term survivors of childhood leukemia. Pediatr Blood Cancer 2015;62:698–703.

37. Drafts BC, Twomley KM, D'Agostino R Jr., et al. Low to moderate dose anthracycline-based chemotherapy is associated with early noninvasive imaging evidence of subclinical cardiovascular disease. J Am Coll Cardiol Img 2013;6:877–85.

38. Jordan JH, Vasu S, Morgan TM, et al. Anthracycline-associated T1 mapping characteristics are elevated independent of the presence of cardiovascular comorbidities in cancer survivors. Circ Cardiovasc Imaging 2016;9:e004325.

39. Lunning MA, Kutty S, Rome ET, et al. Cardiac magnetic resonance imaging for the assessment of the myocardium after doxorubicin-based chemotherapy. Am J Clin Oncol 2015;38:377–81.

40. Heck SL, Gulati G, Hoffmann P, et al. Effect of candesartan and metoprolol on myocardial tissue composition during anthracycline treatment: the PRADA trial. Eur Heart J Cardiovasc Imaging 2018;19:544–52.

41. Muehlberg F, Funk S, Zange L, et al. Native myocardial T1 time can predict development of subsequent anthracycline-induced cardiomyopathy. ESC Heart Fail 2018;5:620–9.

42. Van Vleet JF, Greenwood LA, Ferrans VJ. Pathologic features of adriamycin toxicosis in young pigs: nonskeletal lesions. Am J Vet Res 1979;40:1537–52.

KEY WORDS anthracycline, cardio-oncology, cardiotoxicity, CMR, doxorubicin

APPENDIX For a supplemental table and figure, please see the online version of this paper.